7/7/2014

# KTH - Royal Institute of Technology

DD2402 Advanced Individual Course on Computational Biology


**Author:**

Ioannis Kalfas

MACHINE LEARNING, COMPUTATIONAL BIOLOGY

**Supervisors:**

Bernhard Kaplan, Philip Tully

# KTH - Royal Institute of Technology

**DD2402**

**Advanced Individual Course on Computational Biology**

by Ioannis Kalfas (880918-0592)

Date: 2014-07-07

## 1. Introduction

The goal of this 'Advanced Individual Course' is to get acquainted with a generic memory and neural information processing model, which has been used in a variety of different contexts. For this purpose, it was essential to learn about some basic principles for neural computation, e.g. approaches for modeling neurons and synapses. This report is structured as follows:

First, I will give a basic explanation of neural mechanisms, focusing on the action potential, and then I will describe the Integrate-And-Fire (IAF) neuron model. Emphasis will be given on the concepts of Leaky IAF neuron models with current and conductance based synapses. I will create different plots of the membrane potential of a single IAF neuron by studying the effects of changing different model parameters.

Additionally, I will continue by exploring a specific associative memory model and building a hypercolumnar structure containing several minicolumns and a pool of inhibitory neurons. These columnar structures are considered to be groups of cortical neurons which can be used to model the brain. When they are used in a way to represent the structure and connectivity of neural networks, they create patterns of activity that have actually been observed to happen in the brain. Depending on the cortical model that it used, one can address different parts of the complex functionality of the brain.

### 1.1 Materials and Methods

For the implementation of my experiments, I use Nest 2.2.2 [1] with the Python programming language via the PyNEST extension module. NEST is a simulator for spiking neural network models that focuses on the dynamics, size, and structure of neural networks rather than on the exact morphology of individual neurons. The experienced reader is encouraged to skip the following section.

# 2. Theoretical Background

## 2.1 The Action Potential

An 'action potential' is a short-lasting event in which the membrane potential of a cell rapidly rises and falls, following a consistent, stereotyped trajectory. Typically, a neuron will fire an action potential at the time when its membrane potential, namely the difference in electrical potential between the interior and the exterior of the cell, reaches a threshold value of approximately -55mV. [2]

This event is generated by different types of voltage-gated ion channels which are embedded in a cell's membrane. Various ions (cations and anions), reside both inside and outside of each cell. For neurons, the most prevalent ions are sodium ($Na^+$) and potassium ($K^+$) cations, with the former residing mostly extracellularly and the latter intracellularly. These ions (along with other ions and charged proteins, which are not mentioned for the sake of simplicity) are responsible for keeping the membrane voltage constant at its resting potential, which is typically around -70mV.

An action potential will occur when the channels open after detecting the depolarization stimulus in the transmembrane voltage, and allow an inward flow of sodium ions into the cell. This will cause a more positively charged electrochemical gradient, which produces further rise in the membrane potential, opening more channels, and so on. After a critical threshold, the dominant sodium current will trigger this rapid, stereotyped trajectory of the membrane potential as you can see in the figure below.

During the repolarization phase, the number of open sodium channels is dramatically reduced and the activation of voltage-gated potassium channels is at maximum. At this point in time, the action potential repolarizes beyond the resting membrane voltage (resting state).

The refractory period occurs because most voltage-gated potassium channels are still open, such that the total potassium conductance of the neuron is greater than when the membrane is at its resting steady state. Also, during this period the neuron is insensitive to any input and is not able to fire any other action potentials. Before the membrane potential reaches its resting state, the potassium channels that were opened during the action potential start to close and the membrane potential is determined by the other channels which are normally open at the resting potential.

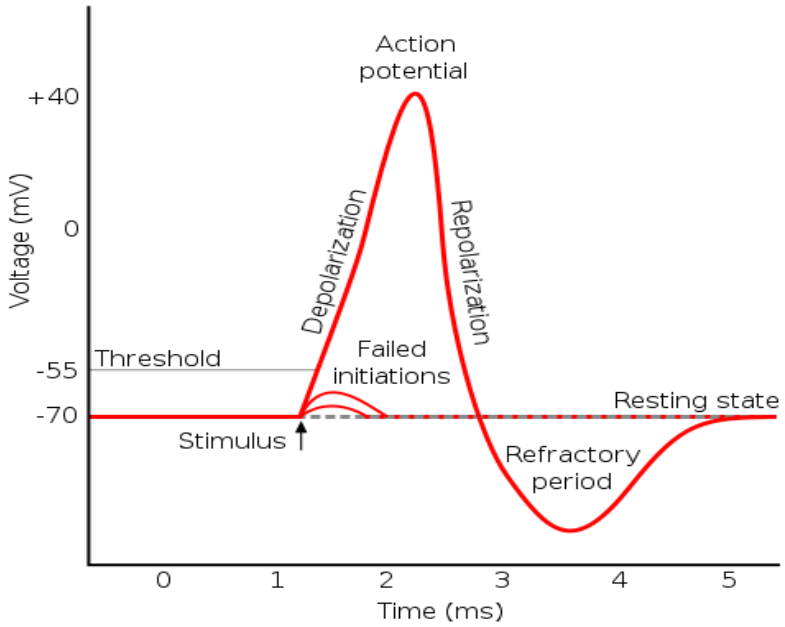


**Figure 1. The Action Potential. The most important event describing how information flows in our brains. [3]**

## 2.2 Integrate-And-Fire neuron model

The integrate-and-fire (IAF) neuron model is one of the most widely used neuron models for modeling the behavior of neural activity. The description of a neuron is done based on its membrane potential, in terms of the inputs it receives from either synapses or injected current [4]. IAF models presume that an action potential occurs when the neuron's membrane potential reaches the threshold value ($V_{th}$). Immediately after, the potential is reset to a Vreset value below the threshold. This represents the refractory period of the action potential, during which the neuron is insensitive to any input and does not fire any other action potentials. Thus, $V_{reset} < V_{th}$. For an animated illustration of the model follow this link.

The IAF model describes a class of neurons and does not include any specific implementation with corresponding equations. One of the first models of a neuron was proposed by Louis Lapicque in 1907, where a neuron is represented in time by:

$$I_e = C_m \cdot \frac{dV_m}{dt}$$

which is the time derivative of the law of capacitance (q = CV). Here $I_e$ is the input current, $C_m$ is the membrane capacitance and $V_m$ the membrane voltage.

# 3. Specific Neuron models and their functions

## 3.1 Leaky Integrate-and-fire with current based synapses

The Leaky Integrate-And-Fire (LIF) model is one of the simplest versions of the neuron models. It can be presented as an electric circuit that consists of a capacitor *C* in parallel with a resistor *R* driven by a current $I_{(t)}$ as explained by Wulfram Gerstner & Werner M. Kistler [11]. This current has two components: $I_{(t)} = I_R + I_C$, where $I_R$ is the current which passes through the linear resistor *R*, and $I_C$ charges the capacitor *C*.
We know from Ohm's law that: $I = \frac{V}{R}$, where V is the resistor's voltage. From the definition of capacity we know that: $C = \frac{q}{V}$, where q is the charge and V the voltage. From the above, we have that: $I_R = V/R$ and $I_C = C \cdot \frac{dV}{dt}$. Thus,

$$I_{(t)} = \frac{V}{R} + C \cdot \frac{dV}{dt}$$

Multiplying the above equation by R and introducing the time constant $\tau_m = RC$, we have:

$$\tau_m \frac{dV}{dt} = -V + R_m I_{(t)}$$

where $\tau_m$ is the membrane time constant of the neuron ($\tau_m = R_m\, C_m$), $R_m$ is the total membrane resistance, V is the membrane voltage and $I_{(t)}$ is the input current. [11] The membrane time constant is a value that is used to describe the rise and fall of membrane voltage and determines how fast the membrane voltage reacts to changes in the input current.

According to P. Dayan and L. F. Abbott [2], focusing on a single compartment neuron, the basic equation describing its circuit is this:

$$c_m \cdot \frac{dV}{dt} = -i_m + \frac{I_e}{A}$$

where $c_m$ is the specific membrane capacitance (capacitance per unit area), $i_m$ is the membrane current per unit area, $I_e$ is the injected current and *A* is the total surface area of the cell. For this model that is analyzed in this section, all the time-independent contributions to the membrane current can be combined together into a single leakage term $i_m = g_L(V - E_L)$, where $E_L$ is the reversal potential which is kept as a free parameter and is adjusted to match the cell being modelled, and $g_L$ is the membrane conductance which is equal to one over the specific membrane resistance ($g_L = 1/r_m$). [2]
In the above equation, replacing $i_m$ with its equivalent $g_L(V - E_L)$ and multiplying with the specific membrane resistance, which is $r_m = 1/g_L$, we get:

$$r_m \cdot c_m \cdot \frac{dV}{dt} = E_L - V + \frac{r_m}{A} I_e$$

Knowing that $r_m \cdot c_m = \tau_m$ and $\frac{r_m}{A} = R_m$(which is the total membrane resistance), we get the following equation which is also implemented in the simulations used later:

$$\tau_m \cdot \frac{dV}{dt} = E_L - V + R_m I_e$$

This equation indicates that when the input current $I_{(t)} = 0$, the membrane potential drops exponentially with time constant $t_m$ to $V = E_L$. [2]

At the point in time when V takes the threshold value $V_{th}$, an action potential will be fired. The membrane voltage will be reset to a value called $V_{reset}$.

The integration part for this model can become clear by considering that each presynaptic spike generates a postsynaptic current pulse. As Gerstner states in [11], if a presynaptic neuron *j* fires a spike at time $t_j^{(f)}$, then a postsynaptic neuron *i* receives a current with time course $\xi(t - t_j^{(f)})$. This will give as a total input current to neuron $i$, the sum over all current pulses,

$$I_j(t) = \sum_j w_{ij} \sum_f \xi(t - t_j^{(f)})$$

One has to consider though, that the amplitude of the postsynaptic current pulse depends on the value of the membrane potential $V_m$ and each spike generated presynaptically will evoke a change in the postsynaptic membrane conductance with a certain time course $g(t - t^{(f)})$ [11]. The postsynaptic current that is generated by a spike at time $t_j^{(f)}$ is thus

$$\xi\left(t - t_j^{(f)}\right) = -g(t - t_j^{(f)})[V_m(t) - E_L]$$

### 3.1.1 Simulated Experiments

In this section, I study the effects of changing the above model's parameters ('iaf_psc_exp' in NEST) in various experimentations. I will shortly explain them under each figure. There can be many parameter changing scenarios, if one considers the weights[1] between the connections and in addition, the different synapse models[2] that can be used. The various parameter changing scenarios, for the present report, will be:

- $C_m$: $C_m$ is the membrane capacity in $pF$.
- $\tau_m = R_m \cdot C_m = \frac{C_m}{g_L}$: $\tau_m$ is the membrane time constant in *ms*, $R_m$ is the membrane resistance in $\Omega$, $C_m$ is the capacity of the membrane in $pF$, $g_L$ is the membrane conductance at rest in $mV$.
- $I_e$ vs. $SpikeRate$: $I_e$ is the constant input current in $pA$.
- Number of spikes for 10 different $V_{reset}$ values (only for the current based model).

[1] The height of the step-increase, when a spike arrives, is called the weight or strength of a synapse and can be modulated by learning rules, and the synaptic time constants. These values determine the impact of a spike on the post-synaptic membrane potential (of the target neuron).

[2] Much more complexity can be introduced by including more details about the synaptic connections between neurons in a network, and experimenting with various synapse models. Some examples are: Static Synapses with homogeneous or heterogeneous weight and delay, Spike-timing-dependent plasticity, Short-term plasticity (Tsodyks & Markram synapses), Neuromodulated synapses, using Dopamine [1].

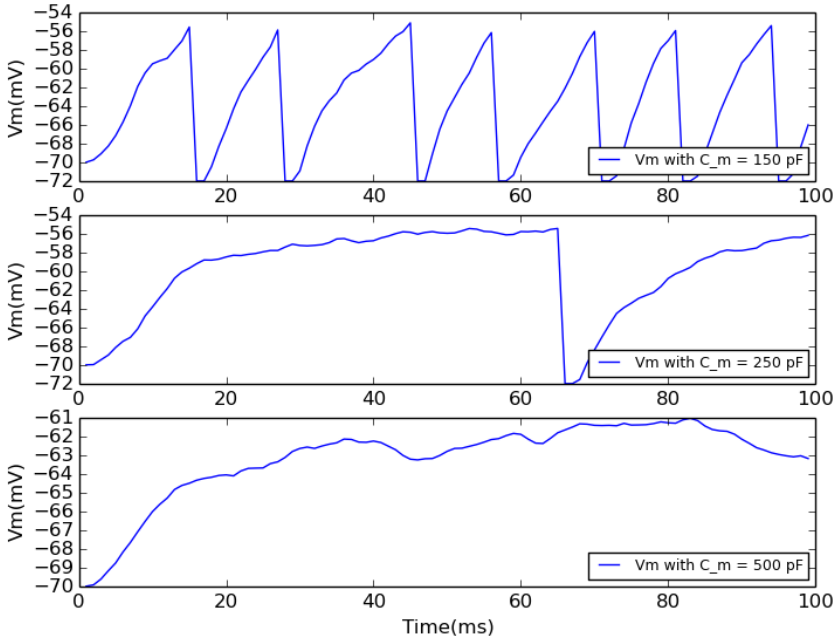


**Figure 2. Changing Capacity. Its default value is 250 $pF$. The input source was Poisson spike trains with a rate of 4500 Hz. Here, we increase its value in three different trials as you can see in the figure. We observe that with greater capacitance the neuron struggles to produce a spike, whereas with decreased capacitance we have a significant firing rate. We understand that when the membrane capacity is lower, the membrane time constant's $\tau$ value is smaller ($\tau = R_m \cdot C_m$). This means that it takes less time for the voltage to increase, therefore it is faster for the neuron to produce spikes. If $C_m$ is small, the neuron membrane can store only a small amount of charge. This is why the membrane potential rises faster and reaches the threshold with less input current.**

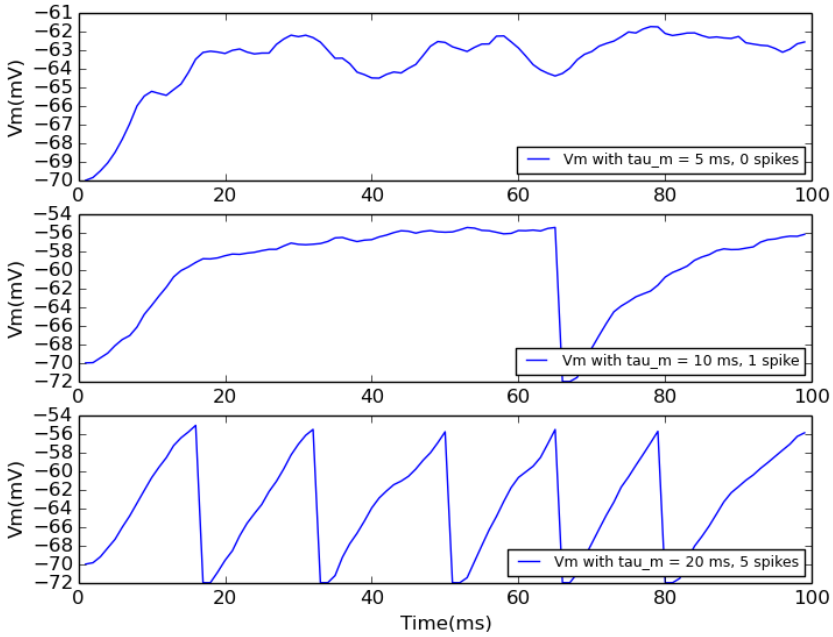


**Figure 3. Changing Time Constant. The default value was 10 *msec*. At the top subfigure, the membrane time constant is halved and in the bottom subfigure, it's value is doubled. This figure can also show the nature of the membrane time constant, meaning that when its value is smaller, then the time it takes for the membrane voltage to increase is smaller and vice versa.**

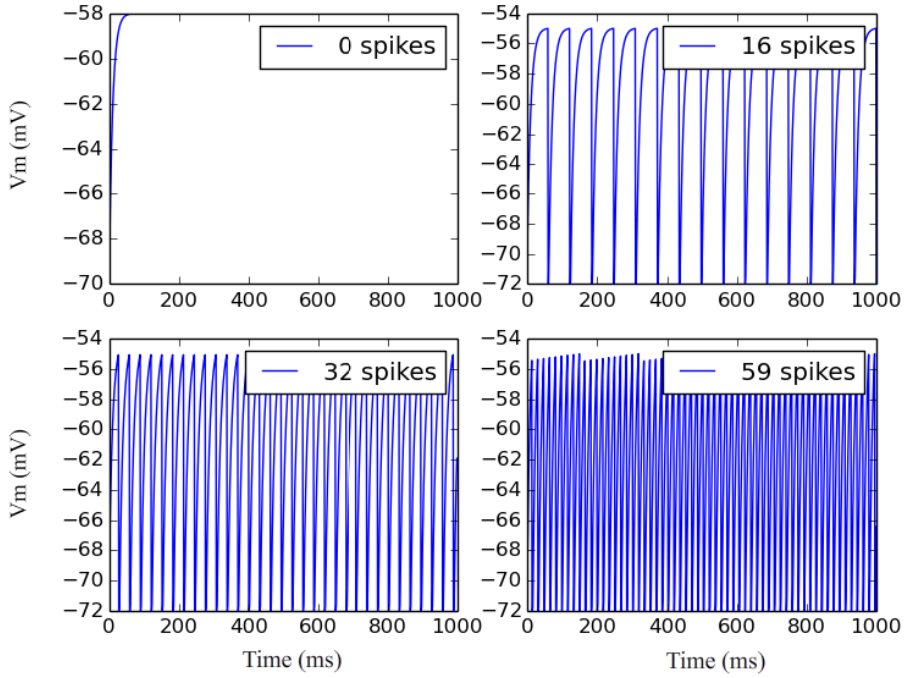


**Figure 4. Looking at the membrane voltage while increasing $I_e$. This is a series of experiments, where I increased the input current in each individual trial and observed the spiking rate values. The exact $I_e$ values can be seen in the figure that follows.**

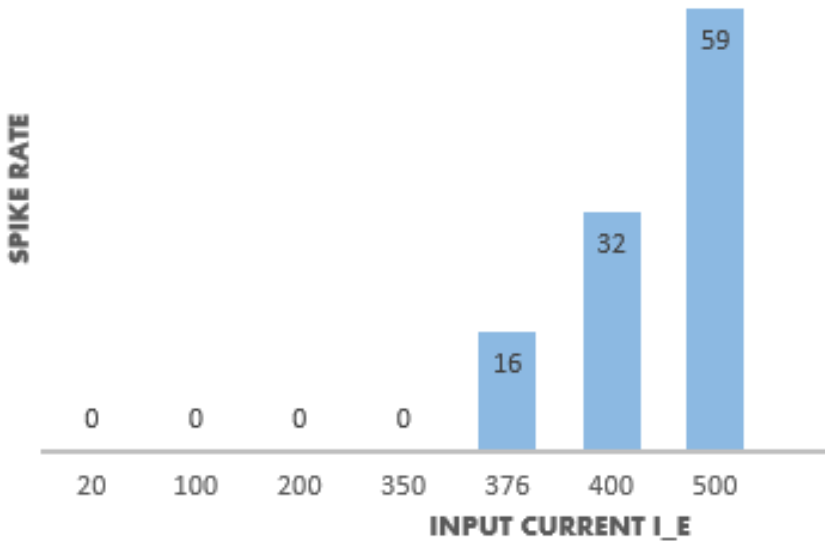


**Figure 5. Spike rate while increasing $I_e$. This is a continuation of the above, but now emphasis is put on the spiking rate instead of the membrane voltage.**

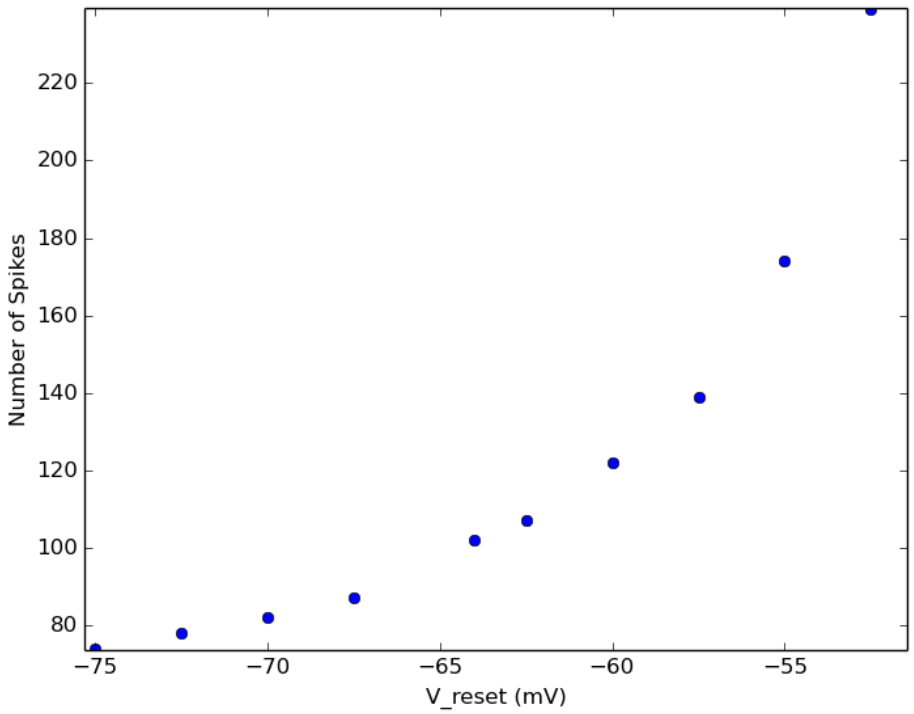


**Figure 6. A number of 1000 Poisson generators (10 Hz) were connected to a single neuron, and by changing its reset Voltage in 10 different trials, the number of produced spikes was recorded in a time frame of 1 second. If $V_{reset} = V_{th}$, the neuron spikes continuously with its maximum firing rate which is $1/\tau_{refrac}$.**

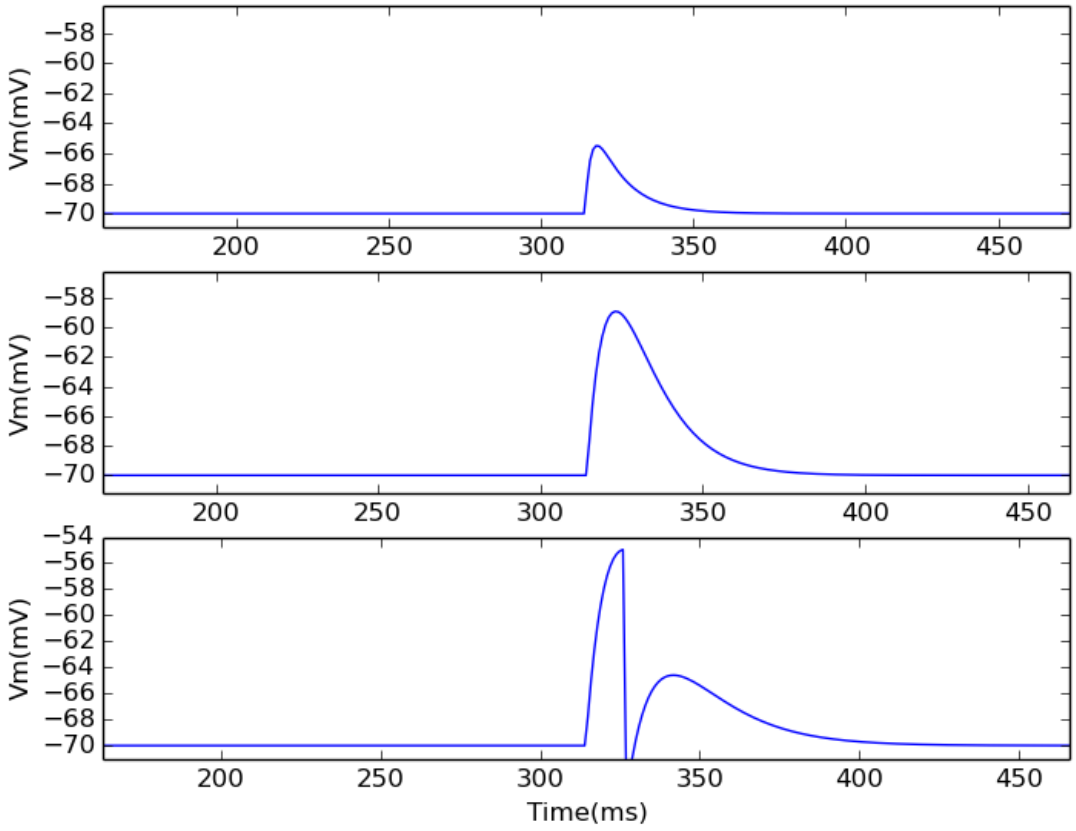


**Figure 7. In this figure, the effects of tau_syn_ex can be observed for a postsynaptic cell that receives one spike at the time of 310 ms. In the top figure tau_syn_ex is 2ms. In the middle figure it is increased to have a value of 8ms and 18ms in the bottom figure. Similar effects can be observed by changing the weights between the neurons, namely, increasing the weights will evoke a larger depolarization of the postsynaptic membrane potential.**

## 3.2 Conductance-Based Leaky Integrate-And-Fire Model

The conductance based LIF model uses a more complex equation to model the impact of an incoming spike. In this model, the effect of an incoming spike is dependent on the membrane potential of the neuron, whereas in the current based LIF model, each spike has the same effect on the membrane potential irrespective of the previous membrane potential. This IF model, includes a passive leak with reversal potential $E_L$ and time constant $\tau_L$. The excitatory/inhibitory synaptic conductances are perceived as Poissonian trains of delta pulses ($P_e$ and $P_i$):

$$\frac{dV}{dt} = -\frac{1}{\tau_L}(V - E_L) - \alpha_e(V - E_e)P_e - a_i(V - E_i)P_i$$

The present model also comprises reversal potential for excitatory/inhibitory synapses ($E_e/E_i$). The $a_e$ /$a_i$ variables are used to define the scale of post-synaptic potential amplitudes. Furthermore, they represent the conductance which is not constant, but follows some time-course described by some function depending on the synapse model. That is when a spike arrives ($P_e! = 0$), $a_e$ follows a step-increase and exponential decay (for exponential synapses, or it follows an alpha-function if an alpha synapse model is used). The time constant for that exponential decay is tau_syn_ex (which I show in "Simulated Experiments" section).

The above parameters give a more realistic view of a biological neuron model by including the main features of dynamic conductance, time constant changes, and voltage-dependent post-synaptic potential amplitudes [5]. Moreover, the conductance based LIF model is able to model so called high- and low-conductance states, and since these states have an impact on the neural processing (e.g. on the temporal resolution, the synaptic efficacies, the responsiveness and gain modulation) and have been seen in in-vivo experiments, this model can be regarded as more biologically plausible [12].

### 3.2.1 Simulated Experiments

Similar experimentations to the LIF current-based model will be performed by changing some parameters on the conductance based LIF model ('iaf_cond_exp' in NEST). The results are similar to the first model qualitatively.

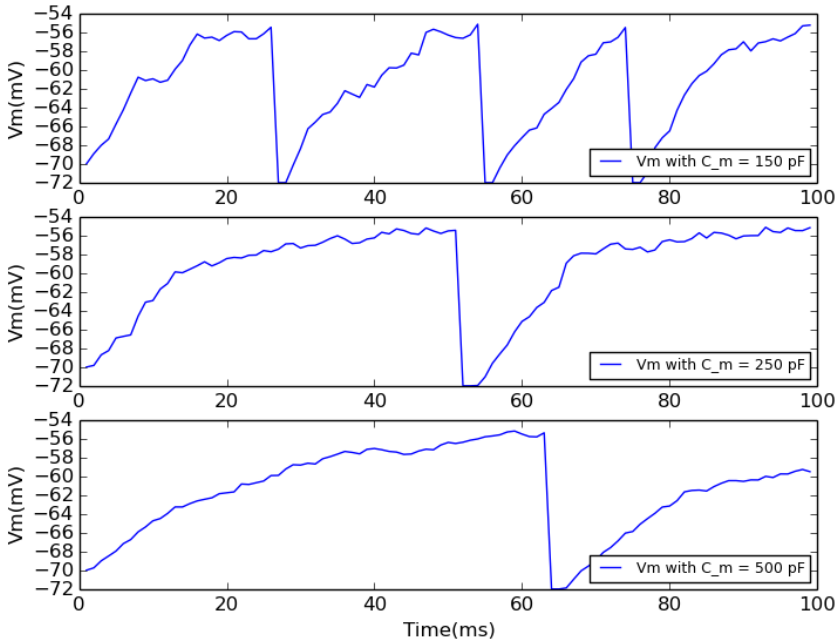


**Figure 8. Changing the cell's Membrane Capacity. Similarly to the LIF model, we observe that with a larger capacity, the neuron does not easily produce a spike and therefore we expect to have less firing rate as it was previously showed for the current based model.**

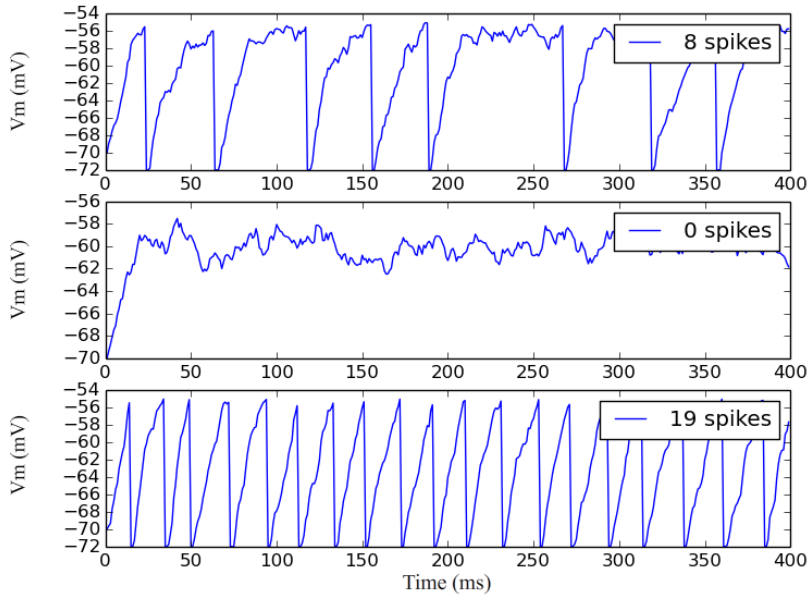


**Figure 9. In this experiment I study the effects of changing the Leak Conductance, which is expressed in the following equation including the membrane time constant and membrane capacitance: tau_m=$C_m/g_L$. The default value of $g_L$ is 16.6667 mV. In this experiment, we initially increase its value by 10 and then decrease its default value by the same amount. We can see from the equation that with larger $g_L$, we get smaller membrane time constant, therefore shorter period of time for which the membrane is depolarized, thus it produces less or no spikes.**

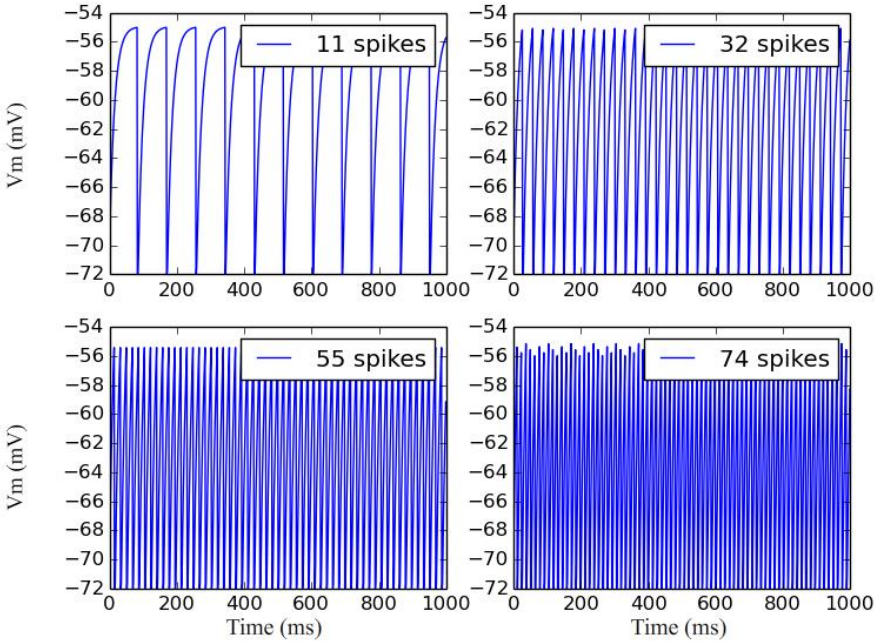


**Figure 10. In this figure (Vm-time) we observe the effect of having an input current I_e just like in the LIF model. The exact I_e values can be seen in the figure that follows.**

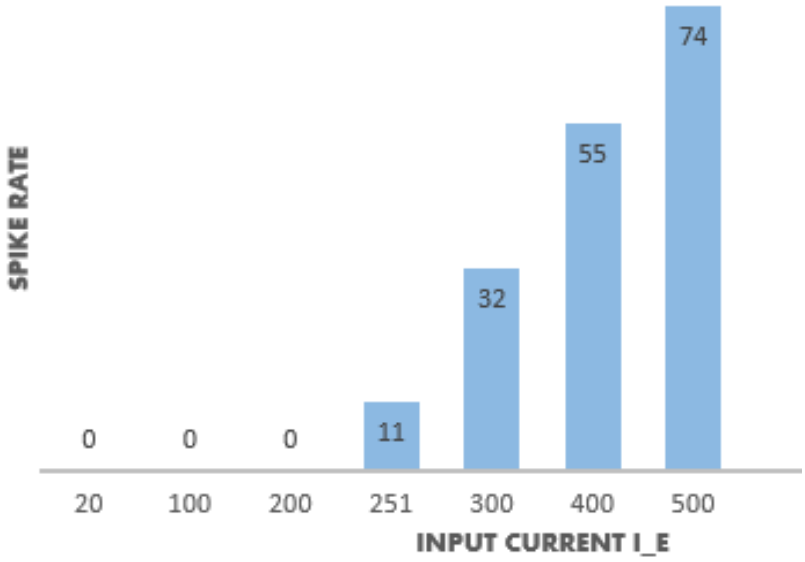


**Figure 11. Just like the previous figure, here we see the effect of an increasing input current I_e emphasizing on the number of spikes produced for each I_e value.**

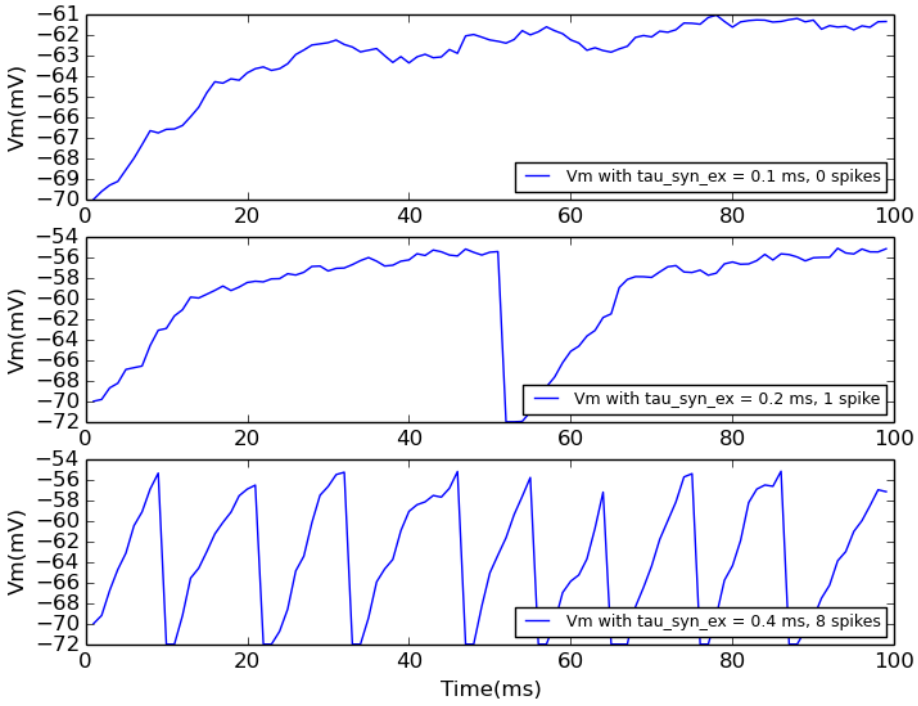


**Figure 12. In the first subplot for this *tau_syn_ex* (excitatory synaptic time constant) experiment, we can see the source's voltage plot and in the following two figures we test two different cases of target neurons connected to the source with excitatory synapses, first tweaking the default value of *tau_syn_ex* from its default 0.2 ms to 0.4 ms and afterwards to 0.1 ms. The Poissonian spike trains used as input had a rate of 4500 Hz.**

## 3.3 Advanced Models with Higher Biophysical Detail

### 3.3.1 Adaptive Exponential Integrate-and-Fire Model

This model is described by Brette and Gerstner [6] as a two-dimensional integrate-and-fire model that combines an exponential spike mechanism with an adaptation equation. Compared to the traditional leaky integrate-and-fire model, it overcomes limitations such as the strict voltage threshold and the current injection and makes use of more realistic mechanisms. For instance, in comparison with previously discussed models, the adaptive exponential IAF replaces the voltage threshold with a smoother spike initiation zone.

The adaptive exponential integrate-and-fire model describes known neuronal firing patterns, e.g., adapting, bursting, delayed spike initiation, initial bursting, fast spiking, and regular spiking [13]. In addition, it makes use of conductance injection which brings the iaf models closer to the real cortical ones.

The membrane potential is given by the following differential equation:

$$\frac{dV}{dt} = -g_L(V - E_L) + g_L\Delta_T\, e^{\frac{V - V_{th}}{\Delta_T}} - g_{e(t)}(V - E_e) - g_{i(t)}(V - E_i) - w + I_e$$

where $g_L$ is the leak conductance, $w$ is the adaptation current, $E_L$ is the leak reversal potential, $\Delta_T$ is the slope factor, and $V_{th}$ is a threshold potential. After a triggering spike, the membrane voltage is reset with $V_{reset} = E_L$ and the slope factor determining the threshold's sharpness. When the slope factor is close to zero, the model becomes the standard iaf model with $V_{th}$.

Now, as far as the adaptation current is concerned, it is defined as follows:

$$\tau_w \frac{dw}{dt} = \alpha(V - E_L) - w$$

where $\tau_w$ is the time constant and $a$ stands for the level of subthreshold adaptation. This equation describes the change of the adaption current with time constant $\tau_w$. The process of spike generation and the upswing shape of the action potential is described by the exponential nonlinearity. The falling phase of the action potential is not described explicitly by the model, but it is replaced by a reset of the voltage to a fixed $V_r$ value [6].

### 3.3.2 Izhikevich Model

Similarly to the previous model, the motivation behind building the Izhikevich model was to try and create a model that would stand as both biophysically realistic and computationally convenient for network simulation. It is a two-dimensional neuron model, that covers the same (if not even more) types of neural firing behaviors depending on the parameters, but is ‘cheaper’ to compute compared to the Adaptive Exponential IAF model, since the differential equation includes a quadratic term instead of an exponential term.

I will not go into much detail for this model since it goes beyond the purpose of this report, but briefly I will state that, it considers the activation of potassium currents and inactivation of sodium currents, in addition to keeping things realistic by including a non-fixed threshold. [7]

### 3.4 Qualitative Comparison

In Figure 13, I present a qualitative comparison of the neuron models I examined earlier in terms of their complexity and how close they are to a real neuron. This figure is a generalization and in no case should it be considered the result of a detailed study.

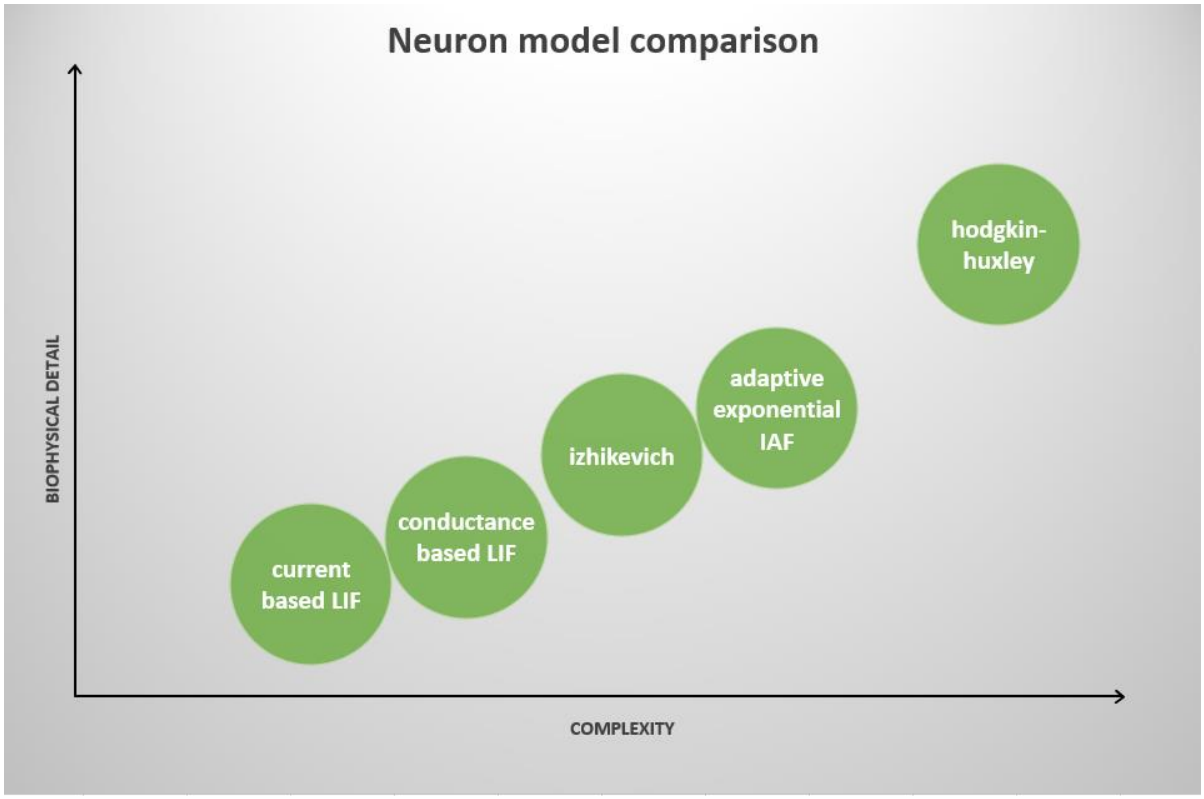


**Figure 13. Qualitative Comparison of different neuron models. The Hodgkin-Huxley model is the one closest to a real neuron.**

# 4. Hypercolumns and Minicolumns

Cortical columns have been suggested to play the role of a canonical microcircuit or elementary cortical processing units in the cortex [14][15][16]. VB Mountcastle, who is often considered the one that invented the term, also gave credit to the earlier work of an American Neuroscience researcher Lorente de Nó for noticing 'vertical chains of neurons' [17]. The functional properties and even the exact shape of these microcircuits in the brain is intensely debated [18].

In this report, I will follow the "column hypothesis" to show how the neuron models described above can be used in simulations for neural networks. I will use the terms of hypercolumns and minicolumns as groups of neurons in the cortex of the brain where minicolumns are thought to encode similar features, whereas a hypercolumn denotes "a unit containing a full set of values for

any given receptive field parameter" [19]. The term 'hypercolumn' was invented to refer to a complete rotation of columns [20]. These structures are believed to stand vertically through the cortex layers. One conclusion that followed various studies on metabolic and electrophysiological studies on cats and monkeys, is that a hypercolumn consists of a number of minicolumns, which is estimated to be from 60 to 80 [16].

Models based on the "column hypothesis" investigate the dynamics of a biophysical model of a piece of neocortex and being set up according to principles suggested by abstract attractor memory models, they are able to perform as an attractor memory [24], [25], exhibiting patterns that are also seen in in vivo experiments.

Minicolumns are also found in the cortex of numerous mammals as an anatomical and functional structure [16]. Their size is much smaller than that of a hypercolumn and they have been found to consist of a number of neurons which has been estimated to be around 80-100 [16]. Again, this number may vary for different cortices. Within the minicolumns one can find both excitatory pyramidal neurons and inhibitory interneurons [8][9][16].

As Johansson C. states at [9], the minicolumns within a hypercolumn express a functional dependency, which means that the output of a hypercolumn results from tight interactions between the minicolumns within it. Furthermore, it is also suggested that there is an inhibitory population comprised of large basket neurons, which are responsible for normalization in the hypercolumns [9].

Upon receiving input, the minicolumns compete with each other for activation and only the one with the highest activation will stay predominantly active, while the others will shut down. Various parameters can be changed, and they might create an obvious strong winner or in some cases, when strong input is given to all the minicolumns, a soft winner. These occurring dynamics follow a known computational principle called "**Winner-take-all**" [10][23]. Winner-take-all networks are frequently used in computational brain models. Recurrent networks that perform a winner-take-all computation are thought to be a basic building block of the cortical microcircuit [22], and they have been used in modelling attention and recognition processes in cortex [21].

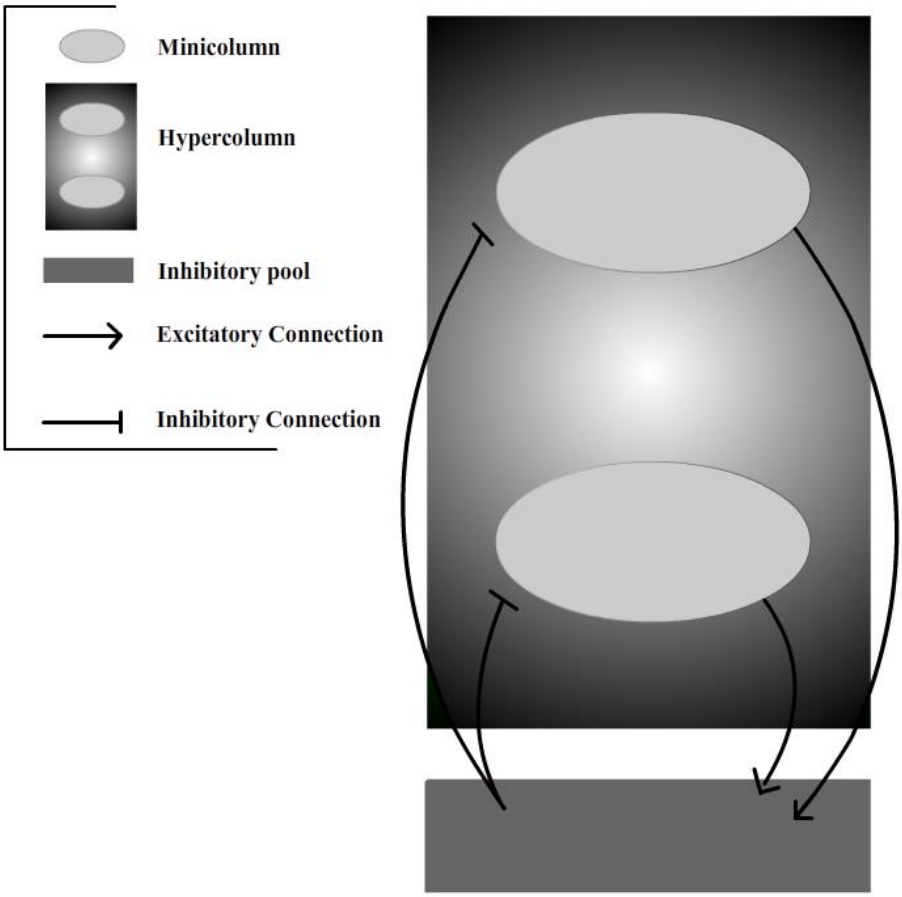


**Figure 14. Simplified Structure of a Hypercolumn with two Minicolumns and an Inhibitory pool.**

## 4.1 A Simple Practical Example of the Hypercolumn

In this section, I will demonstrate the function of a Hypercolumn in terms of its neurons (divided in groups of minicolumns) firing. In the figure below, we can observe three groups of neurons. These groups are the so called minicolumns that I described earlier. Here they consist of 80 excitatory neurons each, and they are all connected to the Hypercolumns' single inhibitory pool (20 neurons) which regulates their excitation. What we can also observe, is the winner-take-all phenomena, which is illustrated as one minicolumn winning in the "firing rate competition" as described earlier. We notice that the top minicolumn (blue group of neurons) that receives the

highest input, is the one with the higher spiking rate, whereas the other minicolumns are either a lot weaker.

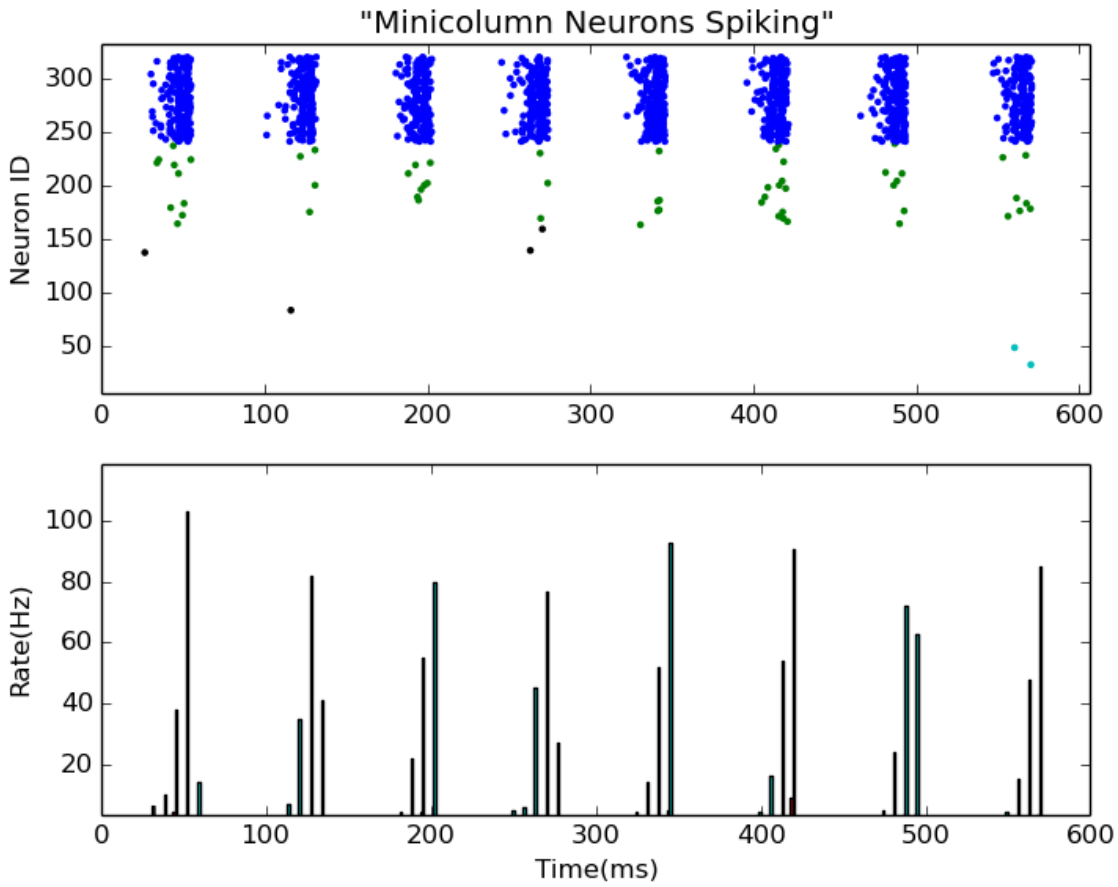


**Figure 15. A Hypercolumn consisting of four minicolumns. Each of the 4 minicolumns has 80 neurons with IDs from 0-80, 81-160, 161-240, 241-320. The inhibitory pool, as mentioned earlier, consists of 20 neurons. The winner-takes-all phenomenon can be observed since one minicolumn prevails in neurons firing to the other two. Inputs were received from Poissonian spike trains with rates in descending order from the top (blue) minicolumn to the bottom (cyan) one: 7000 Hz, 6600 Hz, 6200 Hz, 5800 Hz. Weights from the excitatory cells towards the inhibitory ones have a value of 15. The excitatory cells are connected to the inhibitory pool randomly with a probability of 50%. The weights from inhibitory to excitatory have a value of -10. The inhibitory neurons are connected fully with the excitatory neurons.**

Here, the weights have been increased between the inhibitory population and the minicolumns gradually in 4 trials and record the different spike rates that occur.

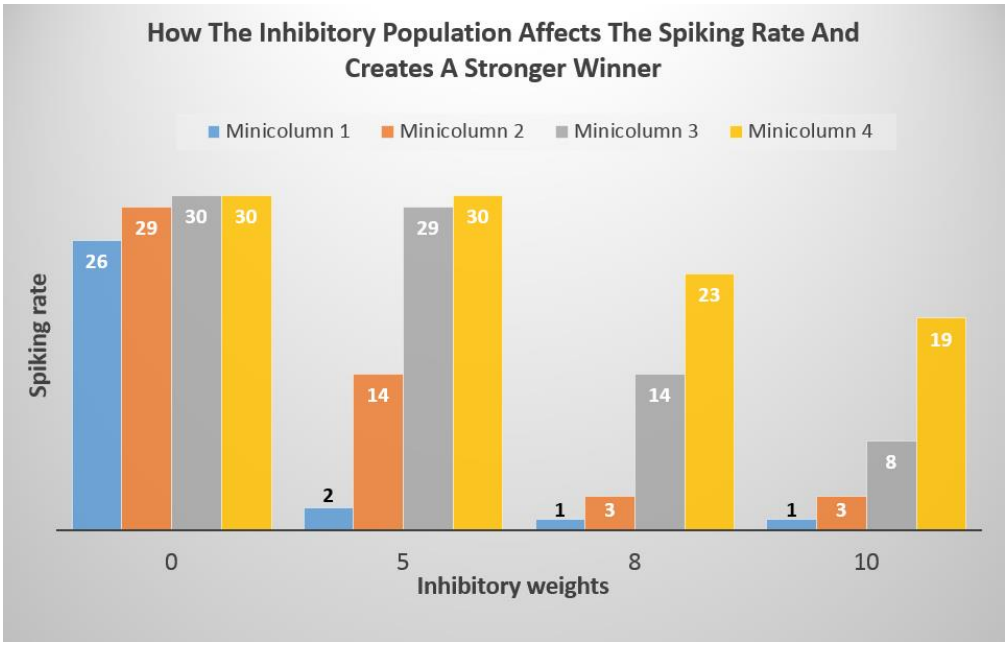


**Figure 15. Minicolumn 1 receives the smallest input and it increases gradually for the rest of them, with Minicolumn 4 receiving the highest input. The "winner" is not obvious with 0 weights, but in later trials it becomes more and more obvious. Increasing the weights more would lead to a small excitation for all the minicolumns, since the inhibition from the basket cell population would become prevalent.**

# 5. Summary / Conclusions

As previously stated in the Introduction section of the present report, the prerequisites to obtain the learning outcome for this course was to familiarize myself with basic principles for neural computation, which I pursued to achieve by studying two IAF neuron models, as well as experiment with simulations of simple neuronal networks using one of these models.

Early in this report, I discussed spike-based communication, a very prominent means of communication in the brain, and went on to describe shortly the theoretical background behind IAF neuron models. Moreover, I studied the effects of changing various parameters of the LIF models with current, and conductance based synapses respectively.

By plotting figures for each individual parameter change, I was able to discern the role of these parameters in the event of spikes firing, in addition to their effect on the neuron's spiking rate. To get a clearer view of how brain computational models work, I followed the "minicolumn hypothesis", created a Hypercolumn consisting of groups of neurons (minicolumns), and observed their firing patterns in parallel to the occurring "winner-takes-all" phenomenon.

# References

[1] Gewaltig M-O & Diesmann M (2007) NEST (Neural Simulation Tool) *Scholarpedia* 2(4):1430.
[2] Dayan, Peter, and Laurence F. Abbott. *Theoretical neuroscience*. Cambridge, MA: MIT Press, 2001.
[3] https://commons.wikimedia.org/wiki/File:Action_potential.svg (current: 06:16, 14 June 2007)
[4] Burkitt, Anthony N. "A review of the integrate-and-fire neuron model: I. Homogeneous synaptic input." *Biological cybernetics* 95.1 (2006): 1-19.
[5] Richardson, Magnus JE, and Wulfram Gerstner. "Conductance versus current-based integrate-and-fire neurons: Is there qualitatively new behavior?"
[6] Gerstner, Wulfram, and Romain Brette. "Adaptive exponential integrate-and-fire model." *Scholarpedia* 4.6 (2009): 8427.
[7] Izhikevich, Eugene M. "Simple model of spiking neurons." *IEEE Transactions on neural networks* 14.6 (2003): 1569-1572.
.[8] Buxhoeveden, Daniel P., and Manuel F. Casanova. "The minicolumn hypothesis in neuroscience." *Brain* 125.5 (2002): 935-951.
[9] Johansson, Christopher. "An attractor memory model of neocortex." (2006).
[10] http://en.wikipedia.org/wiki/Winner-take-all
[11] Wulfram Gerstner & Werner M. Kistler. "Spiking Neuron Models". http://icwww.epfl.ch/~gerstner/SPNM/
[12] Destexhe et al. "THE HIGH-CONDUCTANCE STATE OF NEOCORTICAL NEURONS IN VIVO"
[13] Wulfram Gerstner and Romain Brette (2009) Adaptive exponential integrate-and-fire model. Scholarpedia, 4(6):8427.
[14] Powell, THOMAS PS, and VERNON B. Mountcastle. "Some aspects of the functional organization of the cortex of the postcentral gyrus of the monkey: a correlation of findings obtained in a single unit analysis with cytoarchitecture." *Bull Johns Hopkins Hosp* 105.133-62 (1959).
[15] Mountcastle, Vernon B. "Modality and topographic properties of single neurons of cat's somatic sensory cortex." *J. neurophysiol* 20.4 (1957): 408-434.
[16] Mountcastle, Vernon B. "The columnar organization of the neocortex." *Brain* 120.4 (1997): 701-722.
[17] Lorente de Nó R. (1949). "Cerebral cortex: architecture, intracortical connections, motor projections," in Physiology of the Nervous System, ed. Fulton J. F., editor. (New York: Oxford University Press; ), 288–312
[18] da Costa, Nuno Maçarico, and Kevan AC Martin. "Whose cortical column would that be?." *Frontiers in neuroanatomy* 4 (2010).
[19] Horton, Jonathan C., and Daniel L. Adams. "The cortical column: a structure without a function." *Philosophical Transactions of the Royal Society B: Biological Sciences* 360.1456 (2005): 837-862.
[20] Hubel D.H, Wiesel T.N. Uniformity of monkey striate cortex: a parallel relationship between field size, scatter, and magnification factor. J. Comp. Neurol. 1974b;158:295–305.
[21] Itti, Laurent, Christof Koch, and Ernst Niebur. "A model of saliency-based visual attention for rapid scene analysis." *IEEE Transactions on pattern analysis and machine intelligence* 20.11 (1998): 1254-1259.
[22] Douglas, Rodney J., and Kevan AC Martin. "Neuronal circuits of the neocortex." *Annu. Rev. Neurosci.* 27 (2004): 419-451.
[23] Oster, Matthias, and Shih-Chii Liu. "Spiking inputs to a winner-take-all network." *Advances in Neural Information Processing Systems* 18 (2006): 1051.
[24] Lundqvist, Mikael, et al. "Attractor dynamics in a modular network model of neocortex." *Network: Computation in Neural Systems* 17.3 (2006): 253-276.
[25] Lundqvist, Mikael, Albert Compte, and Anders Lansner. "Bistable, irregular firing and population oscillations in a modular attractor memory network." *PLoS computational biology* 6.6 (2010): e1000803.